JOURNAL OF GEOPHYSICAL RESEARCH, VOL. 107, NO. A12, 1426, doi:10.1029/2001JA000281, 2002

Scale-free statistics of spatiotemporal auroral emissions as depicted by POLAR UVI images: Dynamic magnetosphere is an avalanching system

Vadim M. Uritsky[1] and Alex J. Klimas
NASA Goddard Space Flight Center, Greenbelt, Maryland, USA

Dimitris Vassiliadis
Universities Space Research Association, NASA Goddard Space Flight Center, Greenbelt, Maryland, USA

Damien Chua and George Parks
Department of Earth and Space Sciences, University of Washington, Seattle, Washington, USA

Received 29 August 2001; revised 21 March 2002; accepted 9 August 2002; published 5 December 2002.

[1] We report first results from a spatiotemporal statistical analysis of ionospheric emissions as observed by the Ultraviolet Imager (UVI) onboard the POLAR spacecraft during 4 months of 1997 and 1998. Approximately 12,300 individual emission events near local midnight with durations exceeding the sampling time of the image sequences are investigated. The probability distributions of these events over the lifetime T, maximum area A, integrated area S, maximum power W, and integrated energy output are shown to obey distinct power law relations $p \sim T^{-2.2}$, $p \sim A^{-1.8}$, $p \sim S^{-1.6}$, $p \sim W^{-1.7}$, $p \sim E^{-1.5}$ over a wide range of scales. The observed behavior is consistent with the behavior of statistical−physical avalanche models near a stationary critical state. These results support the hypothesis of self-organized critical dynamics of the magnetosphere and suggest an important role for cross-scale coupling effects in the development of geomagnetic disturbances. *INDEX TERMS:* 2704 Magnetospheric Physics: Auroral phenomena (2407); 2764 Magnetospheric Physics: Plasma sheet; 2772 Magnetospheric Physics: Plasma waves and instabilities; 2788 Magnetospheric Physics: Storms and substorms; 7839 Space Plasma Physics: Nonlinear phenomena; *KEYWORDS:* multiscale turbulence, self-organized criticality, substorms, POLAR UVI experiment

Citation: Uritsky, V. M., A. J. Klimas, D. Vassiliadis, D. Chua, and G. Parks, Scale-free statistics of spatiotemporal auroral emissions as depicted by POLAR UVI images: Dynamic magnetosphere is an avalanching system, *J. Geophys. Res.*, *107*(A12), 1426, doi:10.1029/2001JA000281, 2002.

1. Introduction

[2] Over global spatiotemporal scales, it is well established that Earth's magnetosphere behaves as a low-dimensional dynamical system in response to its solar wind driver [*Sharma*, 1995; *Vassiliadis et al.*, 1995; *Klimas et al.*, 1996; *Pavlos et al.*, 1999a, 1999b; *Sitnov et al.*, 2000; *Gleisner and Lundstedt*, 2001; *Sitnov et al.*, 2002]. A variety of prediction and modeling methods that support or rely on this concept have been developed and applied with considerable success [*Klimas et al.*, 1992, 1994, 1997; *Vassiliadis et al.*, 1995; *Horton and Doxas*, 1996; *Valdivia et al.*, 1996; *Horton and Doxas*, 1998; *Freeman and Farrugia*, 1999; *Valdivia et al.*, 1999; *Vassiliadis et al.*, 1999]. Over small spatiotemporal scales, the magnetosphere tends to demonstrate more complex, and typically unpredictable, dynamics [*Tsurutani et al.*, 1990; *Takalo et al.*, 1993; *Angelopoulos et al.*, 1994; *Borovsky et al.*, 1997] that has been recently identified as the dynamics of a stable critical state of the magnetotail plasma sheet [*Consolini*, 1997; *Uritsky and Pudovkin*, 1998]. In a series of papers, *Chang* [1992a, 1992b, 1998, 1999], *Consolini and Chang* [2001], and *Klimas et al.* [2000a] have shown that these small and large scale dynamics are closely connected. Low-dimensional global dynamics can be a consequence of intrinsically high-dimensional self-organized criticality, or forced self-organized criticality, in the plasma sheet, whereas the high-dimensional plasma sheet component of the dynamics can be controlled by the global loading-unloading magnetospheric dynamics. Due to this intrinsic coupling, understanding the complexity in the magnetospheric behavior associated with critical phenomena appears to be necessary for a correct description of geomagnetic activity as a response to the solar wind driver.

[3] Systems in the state of self-organized criticality (SOC), the main subject of our study, are driven far-from-equilibrium and produce self-similar (i.e., power law) multiscale distributions of individual discharge events, conven-

[1]Now at Institute of Physics, St. Petersburg State University, St. Petersburg, Russia.

0148-0227/02/2001JA000281$09.00

tionally called avalanches [*Bak et al.*, 1987]. The SOC regime is in fact a set of metastable states structured around an attracting critical state [*Bak et al.*, 1988]. In the vicinity of this critical state the system's stochastic dynamics loses its characteristic scales and obeys universal scaling relations [*Robinson*, 1994; *Munoz et al.*, 1999] that considerably simplify its description while providing a chance to better predict its future evolution [*Borodich*, 1997]. A significant body of evidence has been developed that indicates a SOC component in the dynamics of the magnetosphere [*Consolini et al.*, 1996; *Consolini*, 1997; *Uritsky and Pudovkin*, 1998], with much of that evidence indicating that this component is in the plasma sheet [*Angelopoulos et al.*, 1999a, 1999b; *Lui et al.*, 2000]. In this paper we add to this evidence for self-organized criticality in the plasma sheet a result that we find difficult to interpret in any other way. We welcome assistance in finding an alternate explanation.

[4] The approach used in this paper builds on a method introduced by *Lui et al.* [2000] for analyzing some statistical properties of the auroral emissions seen in Polar spacecraft ultraviolet (UVI) images. *Lui et al.* [2000] examined images of the nighttime auroral region from the entire UVI set of January 1997, consisting of 9,033 frames. An intensity threshold well above the instrument noise level was set and individual contiguous emission regions whose intensities were above this threshold were identified. The emitted power and size (area) of each emission region were calculated and recorded. In addition, each of the images was inspected visually to sort them into substorm and quiet time categories. Normalized distributions of emission region size and power were constructed for each of these categories. For both the size and the power distributions in the quiet category, well-defined power law distributions were found. In the substorm category these power law distributions appeared unchanged but a prominent peak corresponding to the largest emission regions was superposed on each. Lui et al. interpreted these results as due to an ever-present component of auroral activity that exhibits scale-free (power law) distributions consistent with SOC regardless of substorm activity, plus well-defined peaks in emitted power and size due to global events during substorm intervals.

[5] We have extended the analysis of *Lui et al.* [2000] from a static spatial analysis to a spatiotemporal analysis of active regions in the Polar UVI images. As we show in the next section, the transition from the spatial (or solely temporal) analysis domain to the combined spatiotemporal domain is crucial for identifying SOC dynamics in a strongly driven system like Earth's magnetosphere. Up to the present, a spatiotemporal statistical analysis of the magnetospheric activity has not been carried out, and so the actual statistical features of geomagnetic disturbances analogous to avalanche activity in SOC models have remained unexplored.

[6] Based on a study of POLAR UVI images of the nighttime ionosphere, we report results from an analysis of probability distributions of spatiotemporal magnetospheric disturbances. We show for the first time that these distributions obey distinct power law relations consistent with SOC theory. The shapes of these distributions are stable and reproducible from month to month. Having been applied to an extensive set of UVI images representing a variety of interplanetary conditions, this analysis reveals no characteristic time, size, or energy scales within the entire available range of studied parameters. During selected intervals of very high magnetospheric activity we observe some deviations of the distribution shapes from pure power law behavior. In the portions of these distributions containing the large events the slopes decrease but no distribution maxima such as the peaks reported by *Lui et al.* [2000] are found. We conclude that the peaks observed by Lui et al. result from an incomplete avalanche detection technique that was limited to a spatial analysis of auroral emissions and missed the temporal component. Our spatiotemporal analysis strongly suggests that the magnetosphere remains in the SOC state for quite different geomagnetic conditions, and that the SOC dynamics encompasses a broad variety of geomagnetic phenomena.

2. Why the Spatiotemporal Approach Is Necessary

[7] SOC systems are known to produce multiscale instabilities called avalanches. In computer simulations of SOC, an avalanche is a group of unstable grid points, or elements of a cellular automaton, that have a single origin of excitation and are contiguous in position and time. The main characteristics of an avalanche, its size and energy, are calculated by integrating over both spatial and temporal coordinates. Power law probability distributions of the avalanches over their size and energy as well as over their lifetime can be interpreted to indicate the closeness of the system to the critical state.

[8] While in SOC models the power law avalanche statistics can be easily verified, in real systems driven by a natural and uncontrollable source this task can be much more complicated and must include elaborate techniques for recognizing individual discharge events. In general, one can distinguish two limiting situations in experimental studies of SOC dynamics, neither of which is realized in the magnetosphere: (1) If the lifetime of the observed events is considerably shorter than the sampling time of the data set, and if the detailed information on spatial propagation of activity is available, then, with certain reservations, the avalanche distributions can be constructed based on the purely spatial analysis. (2) In the opposite case, if the spatial information is not available but the discharge events follow each other in succession so that there are no active regions evolving simultaneously at different spatial locations, some of the avalanche distributions can be obtained from time series analysis of relevant output characteristics of the system. This condition is met if the external driving rate is low compared to the rates associated with the internal dissipation processes, and consequently the frequency of the dissipation events is small.

[9] To understand why this low driving rate condition is not characteristic of the magnetosphere, it is important to recall the meaning of dissipation within the SOC paradigm. Systems that evolve into SOC are subject to loading of a quantity that is conserved except for "dissipation" that may be internal or at the boundaries of the system. It has been suggested [*Klimas et al.*, 2000b] that the relevant conserved quantity in the magnetosphere is magnetic flux and that the dissipation mechanism is localized reconnection in the plasma sheet. The magnetic flux is loaded into the system

from the solar wind and is dissipated internally through annihilation and at the tailward boundary through plasmoid release. Dissipation, in this sense, refers to loss of magnetic flux, not to an energy conversion process.

[10] The direct relationship between localized regions of auroral emission and localized reconnection and plasmoid release in the plasma sheet is now firmly established [*Fairfield et al.*, 1999; *Lyons et al.*, 1999; *Zesta et al.*, 2000; *Ieda et al.*, 2001; *Nakamura et al.*, 2001a, 2001b]. In this paper we show that the auroral emissions, considered as spatiotemporal events, exhibit the statistical properties of avalanches in SOC models. We infer that these statistics are reflections of avalanche like behavior in the plasma sheet involving the localized reconnection regions. In situ plasma sheet observations have revealed that fast flows associated with localized reconnection exhibit some of these statistical properties [*Angelopoulos et al.*, 1999a].

[11] Hypothesizing localized reconnection as the mechanism analogous to internal dissipation in SOC models, we then must ask if the frequency of reconnection in the plasma sheet is sufficiently low to justify the low driving rate condition discussed above. In effect, the low driving rate condition requires that no more than one reconnection site can be active at any given time for the reason that the rate at which magnetic flux enters the magnetosphere is much lower than the rate at which the flux is processed through the plasma sheet at any single reconnection site. However, it appears that the plasma sheet often produces multiple simultaneous reconnection events, most likely because it is close to an instability threshold over an extended spatial region much of the time. The study of *Lui et al.* [2000] demonstrated that at any instant there typically exists more than one active region in the nighttime aurora associated with the plasma sheet.

[12] Therefore, the low driving rate assumption is not satisfied in the magnetosphere and so the results of previously reported time series analyses related to the hypothesis of SOC in the magnetosphere [*Consolini*, 1997; *Takalo et al.*, 1999; *Freeman et al.*, 2000; *Uritsky et al.*, 2001b] are insufficient for obtaining correct avalanche distributions in terms of a rigorous SOC approach. Moreover, since the lifetime of many auroral activations is longer than the sampling time of the UVI image series, the static spatial analysis reported by *Lui et al.* [2000] is also inappropriate. The distributions obtained in that analysis do not represent the statistics of complete events that might be associated with the statistics of SOC avalanches as they are defined in SOC theory and simulations.

[13] The two limiting situations considered above are rarely met in practice. The dynamics of real avalanche systems can usually be found somewhere in between. Real avalanche systems are usually not slowly driven, and the avalanche durations are not infinitesimally short compared to the observational timescale. Using the terminology developed in SOC simulations, such systems are classified as "running" avalanche systems. As our analysis suggests, Earth's magnetosphere is such a system. Although the dynamics of running avalanche systems is rather complex, we are still able to obtain appropriate probability distributions through an investigation of the evolution of the avalanches in both the temporal *and* spatial domains [*Hwa and Kardar*, 1992]. In this way, multiple simultaneous avalanches can be identified and separated and their individual properties tabulated. Recently, this technique was applied to spatiotemporal outputs of a continuum current sheet model by *Klimas et al.* [2000b]. The analysis of the resulting avalanche characteristics enabled a correct identification of the SOC regime in this model notwithstanding the generation of multiple reconnection sites in the current sheet [*Uritsky et al.*, 2001a, 2002].

[14] Up to the present, a spatiotemporal statistical analysis of the magnetospheric activity has not been carried out, and so the statistics of geomagnetic disturbances analogous to avalanche activity in SOC models has remained unknown. In our work, we have successfully applied the spatiotemporal approach to the dynamics of auroral activation regions as represented by Polar UVI images and constructed distribution functions that allowed a straightforward interpretation in terms of the SOC approach.

3. Method

[15] UVI images provide detailed information on the dynamics of spatially distributed magnetotail activity covering extended observation periods. It has been shown that the positions of auroral active regions in the nighttime magnetosphere are correlated with the position of the plasma sheet instabilities [*Fairfield et al.*, 1999; *Lyons et al.*, 1999; *Sauvaud et al.*, 1999; *Sergeev et al.*, 1999; *Ieda et al.*, 2001; *Nakamura et al.*, 2001a, 2001b], whereas timing of the auroral disturbances provides good estimates for both small-scale isolated plasmoid releases [*Ieda et al.*, 2001] and for the global-scale substorm onset times [*Germany et al.*, 1998; *Newell et al.*, 2001]. Depending on the filter used, the brightness of the calibrated UVI images allows remote estimation of different energy characteristics associated with the substorm activity [*Doe et al.*, 1997; *Germany et al.*, 1997; *Chua et al.*, 2001].

[16] Our statistical study was based on an analysis of more than 30,000 POLAR UVI images obtained in January–February 1997 and January–February 1998. The images represent the 165.5 to 174.5 nm portion of the N_2 Lyman–Birge–Hopfield spectral band (LBH-long filter, integration time 36.8 s) which characterizes the energy flux of auroral electrons precipitating into the high-latitude ionosphere [*Germany et al.*, 1994; *Doe et al.*, 1997]. We have studied continuous sequences of the UVI images covering the nighttime sector of the aurora in the magnetic latitude range 55 to 90 degrees and magnetic local times ranging from 2000 to 0400 MLT. The required field of view was usually reached from an altitude above 6 Earth radii where the spacecraft spent about 9 hours per orbit. Images were processed in a magnetic coordinate system.

[17] The sampling time of the images with the chosen filter was 184 s, with the exception of 12 days in January–February 1998 when the instrument was mainly operated in a single LBH-long filter mode, permitting a 37-s temporal resolution. In addition to standard calibration procedures, a dewobbling routine and a line of sight correction were applied to every image to compensate for the nutation of the POLAR spin axis and the Van Rhijn effect, respectively. The image pixels were averaged over square bins of 70 $\times$ 70 km^2 before carrying out the statistical analysis described below. Additional tests have shown that with this spatial

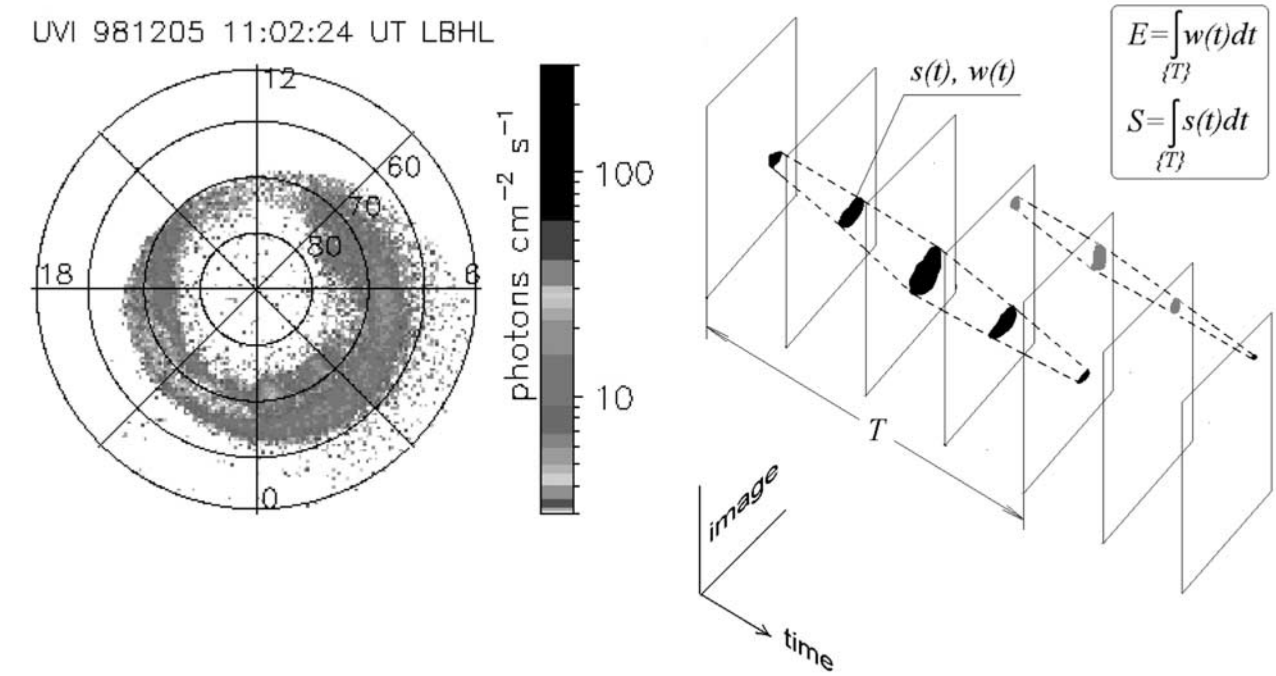

Figure 1. (left) An example of POLAR UVI image. (right) A schematic drawing illustrating the method of identifying spatiotemporal auroral perturbations from POLAR UVI images (spots in the image plane indicate time evolution of two distinct auroral intensification regions with the photon flux exceeding the activity threshold).

resolution, probability distributions similar to those reported below can be obtained using UVI data to which the dewobbling routing has not been applied, and so errors associated with this routine do not affect our conclusions concerning the avalanche statistics of auroral emissions.

[18] To take out the thermal noise in the UVI camera, a set of background subtraction frames was created once per orbit (usually near apogee) and subtracted from the raw images. The remaining noisy pixels that deviate significantly from the counts in a local region of an image were then removed. Since our study was focused on winter months, the day glow contributions to the luminosity of the nightside ionosphere was not significant and thus no day glow correction was applied to the images.

[19] To detect active regions of the aurora, we applied a constant luminosity threshold. The parts of the images with the luminosity values exceeding the threshold were considered active and treated as instant "snapshots" of spatiotemporal geomagnetic perturbations projected to the aurora. We studied the evolution of those events that lasted longer than the image sampling interval and so persisted in at least two successive frames. To identify the spatiotemporal trace of the events, we used an explicit geometric technique that consisted of checking the intersection (in terms of common pixels projected in a magnetic coordinate system) of the perturbed areas in every pair of consecutive frames following the snapshot containing the origin of the perturbation (Figure 1). The time horizon for this search was limited to 5 hours, which is about half of the typical duration of the continuous data segments available. The perturbations that exceeded this limit or were interrupted by a gap in the image sequence that was longer that 3 sampling intervals have been removed from further analysis. During storm and substorm times, the active auroral areas can split and/or overlap constituting complex dynamical patterns. These uncertainties were resolved based on the definition of avalanches used in running cellular automaton models of SOC [*Becker et al.*, 1995]. Namely, the split perturbations with a unique source were considered parts of a single event, the merged perturbations with spatially distinct

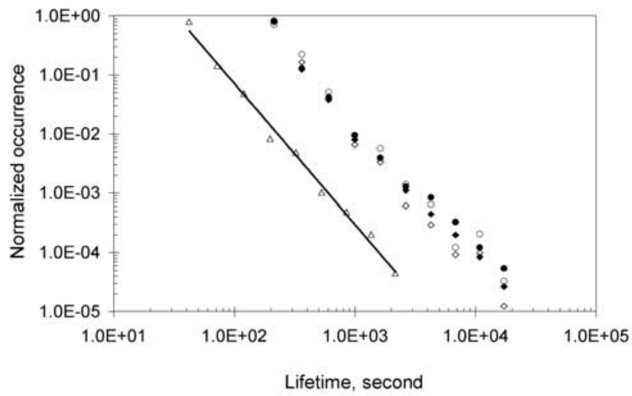

Figure 2. Lifetime probability distributions of spatiotemporal auroral perturbations obtained for January 1997 (solid circles), February 1997 (solid diamonds), January 1998 (empty circles) and February 1998 (empty diamonds) using UVI images with 184-s temporal resolution. Empty triangles correspond to the distribution plot built using 37-s resolution image sequences collected in January and February 1998 in the single LBH-long filter mode.

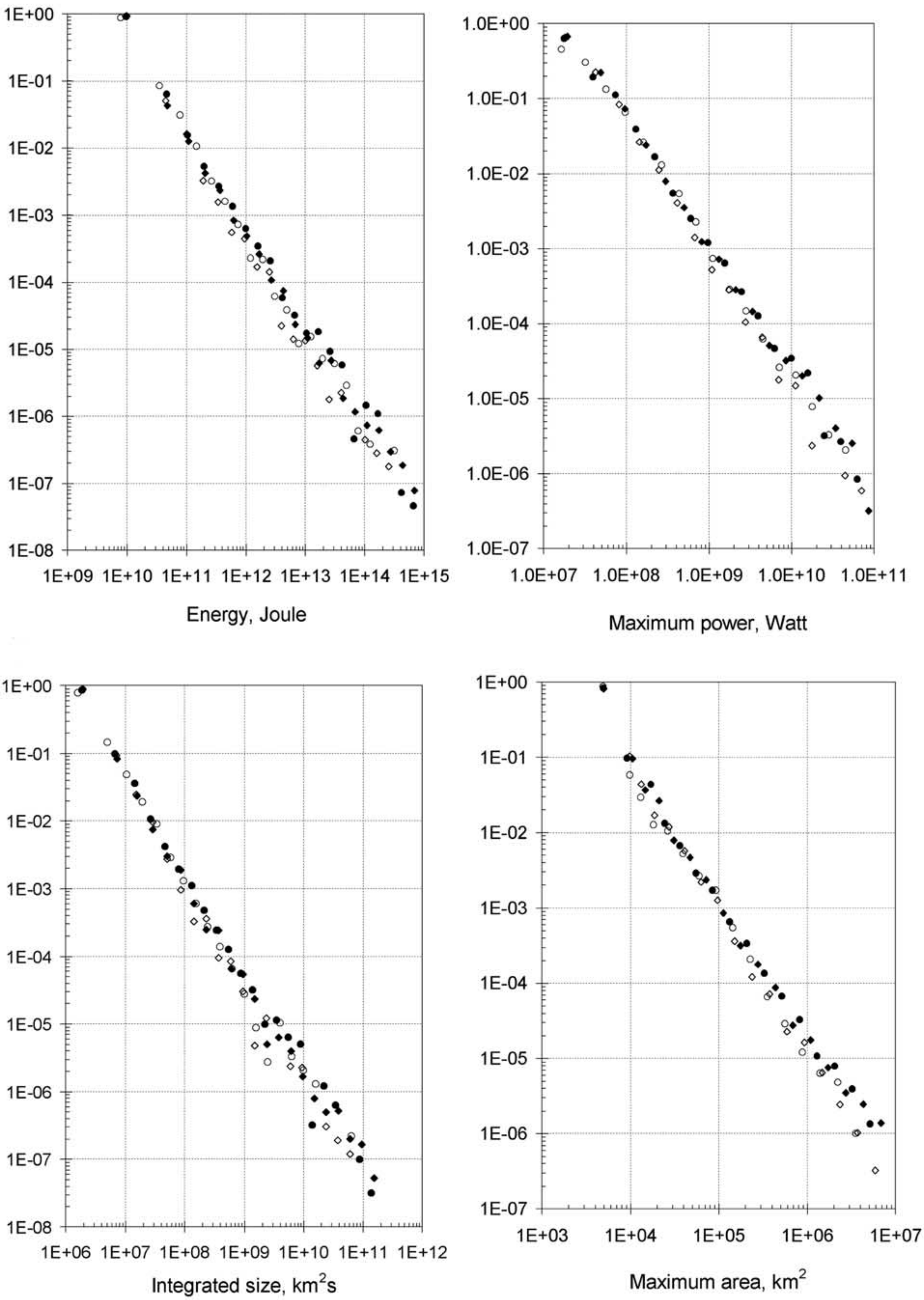

Figure 3. Normalized occurrence of spatiotemporal auroral perturbations as a function of maximum area A, maximum power output W, integrated size S, total energy deposition by auroral electrons E (resolution 184 s). Specification of months is the same as in Figure 2.

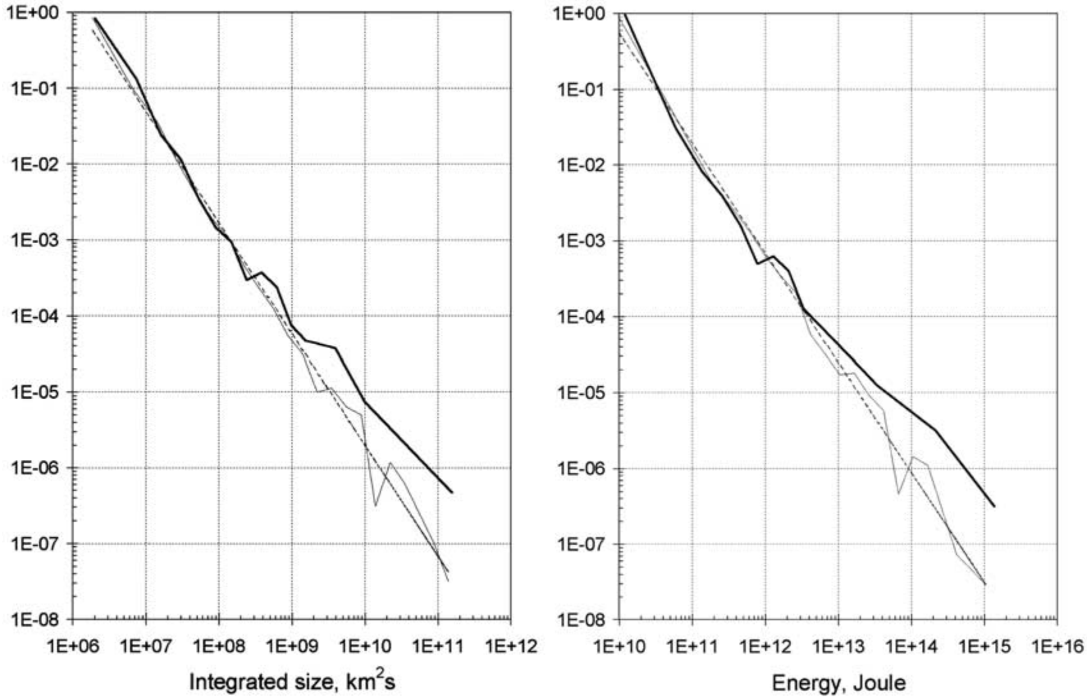

Figure 4. Probability distributions $p(S)$ and $p(E)$ characterizing dynamics of auroral active regions during the major magnetic storm of 10–11 January 1997 (thick lines) and the entire month of January 1997 (thin lines). The straight dashed lines show the average slopes of the distributions for the entire month.

origins were treated as separate ones (the common "tail" following the merging event was ascribed to the perturbation that started earlier).

[20] In total, about 12,300 auroral events were detected using the technique described above. After each event was identified, we calculated its lifetime T defined as the interval between the start and end times of the event (see Figure 1), as well as its integrated size S and its integrated energy E, defined as

$$S = \int_{\{T\}} s(t)dt; \qquad E = \int_{\{T\}} w(t)dt \tag{1}$$

where $s(t)$ and $w(t)$ are correspondingly the area of the perturbation and the energy deposition into this area by auroral electrons at time t and integration is done over the lifetime of each event. To compute $w(t)$, we converted LBH-long photon fluxes of a given UVI image to energy fluxes in terms of Joules $\cdot$ cm^{-2} $\cdot$ s^{-1} using the proportionality constant of $2.74 \cdot 10^{-8}$ Joule $\cdot$ photon^{-1} [*Brittnacher et al.*, 1997; *Carbary et al.*, 2000], and then integrated the obtained values over the perturbation area $s(t)$. The applied conversion is based on the fact that the LBH-long flux is directly proportional to energy flux with only a weak dependence on the mean energy of the incident electrons.

[21] Formally, the quantity S in (1) corresponds exactly to the avalanche size as it is determined in SOC models, and E can be considered as the energy output of the avalanches. In addition, we estimated the maximum active surface area A and maximum energy deposition rate W due the perturbation.

[22] To study the statistics of the auroral events, we calculated their normalized occurrences p for different T, S, E, A and W values. The probability distributions were averaged over exponentially increasing bins to ensure equidistant steps (about 5 per decade) on a logarithmic scale.

4. Results and Discussion

[23] The results of the statistical analysis of the auroral events detected using the luminosity threshold of 10 pho-

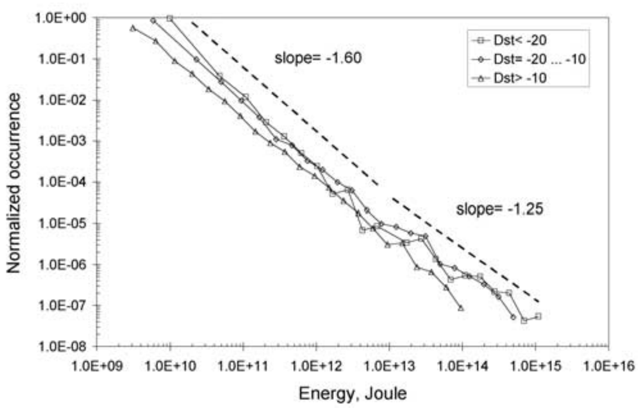

Figure 5. Distribution of auroral events over the energy E for three characteristic ranges of the D_{st} index (in nT). The slope values shown correspond to the condition $D_{st} < -10$ nT, the transition between the two slopes occurs around $E = 10^{13}$ Joules. A similar tendency (appearing of two power law exponents during high geomagnetic activity periods) can be revealed in $p(S)$, $p(A)$ and $p(W)$ distributions.

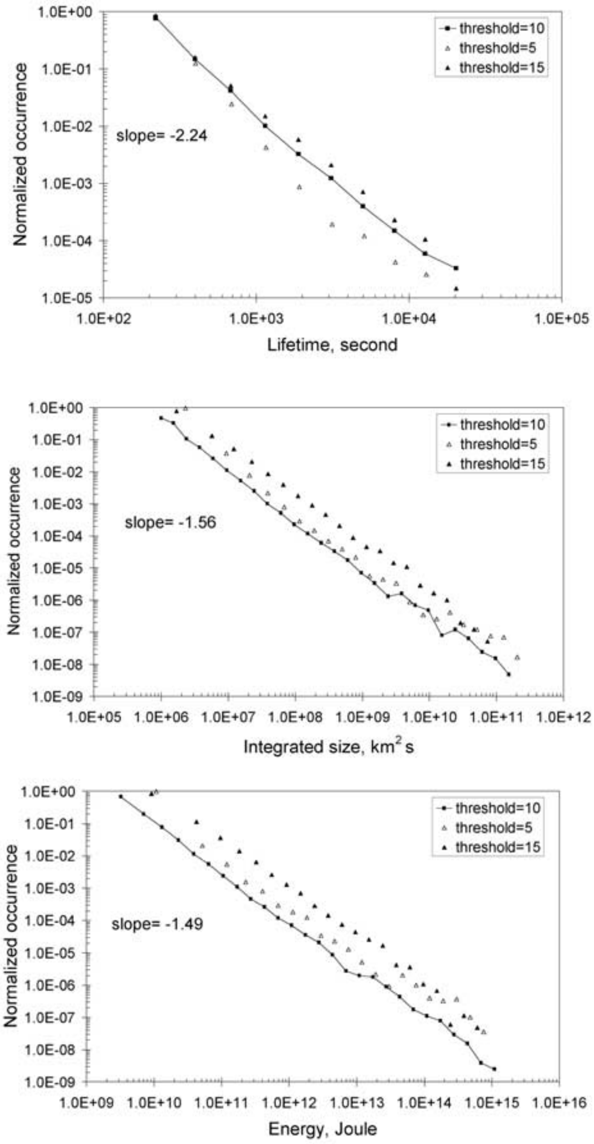

Figure 6. Averaged probability distributions of the auroral perturbations obtained for the entire period of study using three levels of the activity threshold (in photons $\cdot$ cm^{-2} $\cdot$ s^{-1}). The slope exponents are estimated for the threshold of 10 photons $\cdot$ cm^{-2} $\cdot$ s^{-1}.

tons $\cdot$ cm^{-2} $\cdot$ s^{-1}, which is approximately twice the level above which the counts in the UVI images become statistically significant, are presented in Figures 2–5. The results for two other luminosity thresholds, 5 and 15 photons $\cdot$ cm^{-2} $\cdot$ s^{-1}, are presented in Figure 6 and shown to be similar to the results for the threshold of 10 photons $\cdot$ cm^{-2} $\cdot$ s^{-1} that we discuss here.

[24] Figure 2 shows lifetime probability distributions constructed using image sequences collected with standard (184-s) and high (37-s) temporal resolution. The resulting plots show distinct power law behavior. The distribution obtained from high-resolution data, thus allowing more accurate identification of the auroral perturbation timing, looks somewhat more stable compared to the distributions obtained using 184-s resolution data on a month-by-month basis. However, the low-resolution data has the same (within the limits of statistical error) value of power law exponent as the exponent from the high-resolution data, and so can be considered a reasonable approximation to the occurrence probabilities. The entire range of lifetimes consistent with the power law behavior of the lifetime distribution lies between about 1 minute and 5 hours thus involving effectively all relaxation timescales associated with substorm activity.

[25] The distributions of the auroral events over other calculated parameters are shown in Figure 3. The plots were constructed separately for each month using 184-s-resolution image sequences since they were the dominant portions of the available data. Both the integrated and extremal size and energy characteristics of the auroral events have well-defined power law statistics over a broad range of scales. This range seems to be limited only by physically or technically accessible values of the studied parameters. Indeed, the left bounds of $p(A)$, $p(W)$, $p(S)$, and $p(E)$ plots are determined respectively by the spatial resolution of the images (we used the pixel size of $4.9 \cdot 10^3$ km^2), the chosen luminosity threshold which corresponds to the minimum power output in a single pixel of $1.3 \cdot 10^7$ Watt, the product of the pixel area and the sampling time ($9.0 \cdot 10^5$ km^2 $\cdot$ s), and the product of the minimum power output and the sampling time ($2.4 \cdot 10^9$ Joule). The right bounds of the distributions are roughly given by the entire area of the studied sector of the auroral oval (about $2 \cdot 10^7$ km^2), the maximum power of the auroral electrons precipitating during major storm (of the order of 10^{11} Watt), the product of the maximum integration time and the maximum area ($2 \cdot 10^{11}$ km^2 $\cdot$ s), and the product of this time with the maximum power ($2 \cdot 10^{15}$ Joule). The observed maximum perturbation energy is in agreement with the AE-index-based estimation of the electron precipitation energy due to large substorms ($2 \cdot 10^{15}$ Joule [*Weiss et al.*, 1992]).

[26] The shapes of the probability distributions referring to different periods of study look rather similar, although the distribution slopes were inconsiderably but systematically steeper in February–January 1998 compared to the same months of 1997 (Table 1). The observed change in slopes can reflect essentially different interplanetary conditions during the two time intervals and, if this interpretation is correct, it indicates a possibility of using the distribution exponents for quantifying the global geomagnetic response. Independent of the observation period, we found no statistically significant "bump" on the right-hand portions of the distribution functions referring to strong magnetospheric activity. However, we noticed that the slopes of this part of the distributions tended to be lower than the average slopes specified above in the periods when the activity became exceptionally high. As an example, we have considered the statistics of auroral active regions during a major magnetic storm that occurred in 10–11 January 1997. A comparison of these statistics with those obtained before for the whole of January 1997 demonstrates that the magnetic storm manifested itself in a "break" of the distribution curves $p(S)$ and $p(E)$ (Figure 4). The slopes at the right side of the break are lower than the ones at the left side, the latter being close to the power law exponents characterizing the entire month.

[27] To assess more systematically the influence of the geomagnetic activity on the power law distributions of

Table 1. Power Law Exponents (Mean Value ± Standard Error) of the Probability Distributions of Auroral Events During Four Studied Time Intervals

Observation Period	$p(T)$	$p(A)$	$p(W)$	$p(S)$	$p(E)$
January 1997	2.08 ± 0.12	1.73 ± 0.03	1.66 ± 0.03	1.45 ± 0.04	1.46 ± 0.04
February 1997	2.21 ± 0.11	1.74 ± 0.03	1.68 ± 0.03	1.51 ± 0.03	1.39 ± 0.02
January 1998	2.24 ± 0.11	1.81 ± 0.04	1.73 ± 0.02	1.62 ± 0.02	1.62 ± 0.03
February 1998	2.39 ± 0.11	1.92 ± 0.04	1.82 ± 0.03	1.63 ± 0.06	1.61 ± 0.04

auroral emissions, we considered the mean value $\overline{D_{st}}$ of the D_{st} index averaged over the lifetime of each event. Based on this parameter, the whole set of the detected events was divided into three groups: the events that evolved during relatively low magnetospheric activity ($\overline{D_{st}} > -10$ nT), the events observed in the intermediate activity periods (-20 nT $< \overline{D_{st}} < -10$nT), and the events associated with strong activity ($\overline{D_{st}} < -20$ nT) The statistical study has shown that the most stable power law distributions were observed during quiet times, whereas intermediate and active periods are associated with a break on the distributions (Figure 5) similar to the break in Figure 4. This implies that the statistics of large ionospheric perturbations is also power law in form but characterized by a somewhat lower slope compared to the statistics of smaller events. The transition between these power law behaviors occurs around 10^{13} Joules in terms of the integrated energy E of precipitated electrons. Recently, *Carbary et al.* [2000] have estimated the total energy of precipitating electrons of substorm features observed in the LBH-long band of Polar UVI images during distinctive substorms of January 1997. Using a frame-by-frame analysis of auroral active regions (“blobs”) similar to the analysis applied in our study, they have found that the average emission energy associated with substorm development is about $2 \cdot 10^{13}$Joules, the value close to the position of the break on the distribution plots in Figure 5. This fact indicates that the lower and the higher slopes seen in Figure 5 may represent the statistics of large and small substorms, correspondingly.

[28] It must be emphasized that even during the highly perturbed periods of magnetospheric dynamics, we see no distribution maxima such as maxima reported by *Lui et al.* [2000]. We propose that the “bumps” on the distributions observed by Lui et al. during magnetospheric substorms do not represent actual characteristic scales of auroral activations considered as SOC avalanches but have an entirely methodological origin. Namely, with the exception of very short emissions, the auroral blobs seen around the same location in several consecutive UVI frames usually reflect different phases of the same perturbation. When treated as independent statistical events as was done by Lui et al., such blobs lead to overestimating the occurrence of large (and prolonged) auroral activations thus creating an artificial peak on the distribution curves during substorm intervals. Our results demonstrate that this peak is not observed when more appropriate spatiotemporal technique is applied, and so the magnetosphere is likely to display a SOC-like behavior for quite different geomagnetic conditions, magnetospheric storms and substorms included.

[29] As numerical simulations of SOC suggest, to verify the hypothesis of SOC in the magnetosphere in a more rigorous way we need to study a sufficiently large set of geomagnetic responses *without* differentiating between periods of time dominated by large or small activity. When the system is driven by nonstationary input—the situation typical for the magnetosphere and, in particular, for the magnetotail plasma sheet—the simultaneous analysis of a mixture of all possible driving conditions and modes of response becomes a must. It is only this approach that encompasses the full spectrum of system activity and leads to representative avalanche distributions. In the SOC state, these distributions are expected to be power law in form, no matter how diverse the individual events contributing to the statistics. Even if some of the transient regimes of a dynamically driven system exhibit deviation from a pure scale-free behavior, the system is considered to be in or near

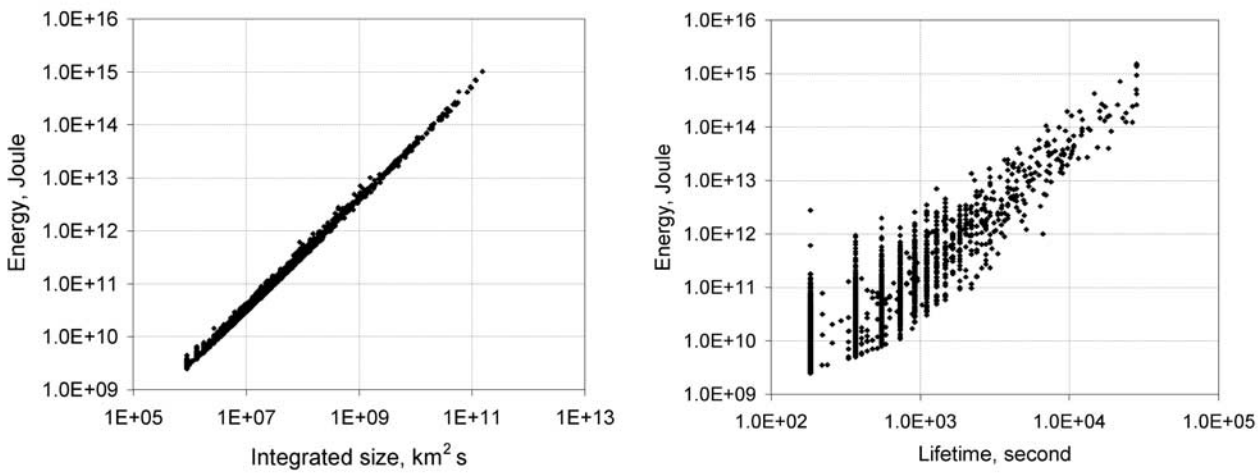

Figure 7. Scatterplots of auroral event energy as a function of the integrated size and the lifetime.

the SOC point if the overall analysis reveals distinct and robust power laws in the probability distributions.

[30] Accordingly, we have applied our distribution analysis to all of the events detected during the four studied months taken together. The resulting histograms have a remarkably stable power law form over at least five orders of magnitude. The shape and the slope values of the $p(S)$ and $p(E)$ distributions do not vary significantly as the threshold applied for determination of active auroral regions changes within the range 5 to 15 photons $\cdot$ cm^{-2} $\cdot$ s^{-1} (Figure 6). The lifetime distribution $p(T)$ remains stable within the range 10 to 15 photons $\cdot$ cm^{-2} $\cdot$ s^{-1}. The steeper slope of $p(T)$ for the threshold 5 photons $\cdot$ cm^{-2} $\cdot$ s^{-1} arises because the determination of active periods at low activity is affected by noise, and so it has a methodological origin. It is important to emphasize that the statistics presented in Figure 6 combine quite different magnetospheric conditions. In particular, they include several storm and strong substorm events characterized by crossover effects similar to that in Figures 4 and 5. Nevertheless, the whole dynamics comprising all levels of magnetospheric activity remains scale-invariant indicating that those extreme events take their place in the statistical hierarchy underlying the power laws without violating them.

[31] Based on this result, we arrive at the main conclusion of this study; the dynamic magnetosphere, as represented by the spatiotemporal evolution of auroral emissions, does operate in a self-organized critical state.

[32] Despite the fact that power law distributions are quite common in nature, the observed range of scale-invariance in the $p(S)$ and $p(E)$ distributions is remarkable. One famous example of such broadband self-similarity is the famous Gutenberg–Richter empirical relation describing the power law statistics of seismic events with different magnitudes [*Turcotte*, 1997]. Some other examples are the cosmic ray energy spectrum [*Cronin*, 1997], probability distribution of US forest fires [*Malamud et al.*, 1998], and solar flares statistics [*Charbonneau et al.*, 2001]. The broadband self-similarity is commonly associated with some scale-invariant physical mechanism, and one of the most universal, straightforward, and robust such mechanisms is presented by SOC. However, more typically the range of scale-free behavior in natural systems is narrower due to unavoidable finite-size effects. A possible reason for this wide range in the magnetosphere is that a huge number of degrees of freedom are involved in the dynamics of the magnetotail plasma sheet due to its continuum nature and its vast spatial extent. The actual range of power law statistics can be even broader than that shown in Figure 5 since the analysis of the smallest auroral disturbances was limited by the available image resolution.

[33] In addition to the probability distribution analysis, we have studied the dependence of the energy E of auroral perturbations on the perturbation lifetime T and on the integrated size S. Scatterplots (Figure 7, luminosity threshold 10 photons $\cdot$ cm^{-2} $\cdot$ s^{-1}) have revealed that the perturbation energy is directly proportional to S (although the instantaneous w/s ratios varied dramatically) and scales with T as $E \sim T^{(1.8 \leftrightarrow 2.2)}$. The first of these relations ($E \propto S$) is characteristic of many cellular automaton models displaying SOC, including the prototypical sandpile model [*Bak et al.*, 1988]. The second relation is in agreement with so-called spreading experiments in systems with spatially extended degrees of freedom [*Munoz et al.*, 1999] and also indicates that the dynamics of the auroral perturbations corresponds well to avalanche dynamics at criticality (see also the recent results on the analysis of the spreading exponents in the electrojet index dynamics [*Uritsky et al.*, 2001b]). Extremal characteristics of auroral events—maximum active surface area A and maximum energy deposition rate W due the perturbation—displayed almost no correlation with T and scaled approximately as a square root of S and E, the observation being in agreement with the other power law relations discussed above.

5. Conclusion

[34] We have reported results from a spatiotemporal statistical analysis of ionospheric emissions as observed by the Ultraviolet Imager (UVI) onboard the POLAR spacecraft during four months of 1997 and 1998. Based on our investigation of approximately 12,300 individual emission regions near midnight with durations exceeding the sampling time of the image sequences, we have constructed probability distributions of multiscale activity of the types that have recently been associated with the dynamics of nonlinear statistical–physical models with many degrees of freedom in the vicinity of the self-organized critical state.

[35] We have revealed that the probability distributions of spatiotemporal auroral perturbations are essentially scale-free, with no characteristic activity size in terms of duration, area, or energy output. The observed power laws are robust with respect to variations of the activity threshold, and seem to be limited only by the range of scales available in the data. In particular, this range involves remarkably broad (more than five decades) intervals of energy output and integrated size of auroral emissions. The power of the auroral electron precipitation is known to be linearly related to the auroral electrojet index which in its turn is proportional to the power of the ionospheric Joule heating, one of the major mechanisms of substorm energy dissipation [*Weiss et al.*, 1992]. These relationships suggest that the overall energy output from magnetotail disturbances during substorms may also obey power law statistics. In this sense, the energy probability distribution can be viewed as an analogue of the famous Gutenberg–Richter relation describing the statistics of seismic events with different magnitudes [*Main*, 1996].

[36] The observed power law statistics are consistent with the behavior of numerical models operating near the SOC limit; these statistics provide important observational evidence for stationary critical dynamics in the magnetosphere. Based on this result, one can expect cross-scale coupling effects to play a significant, if not crucial, role in the development of geomagnetic disturbances. More specifically, the SOC principle implies that large-scale properties of the magnetotail plasma sheet depend critically on the statistical hierarchy of small- and intermediate-scale perturbations associated with sporadic localized magnetic reconnections, current sheet disruptions, and other localized plasma instabilities [*Klimas et al.*, 2000b]. The global stability of the plasma sheet requires that these local events self-organize into scale-invariant dynamical patterns char-

acterized by algebraic probability distribution functions with certain values of power law exponents; the global stability cannot be maintained if this condition is not satisfied. In principle, this requirement provides a way to understand the transition in the plasma sheet from sporadic, localized reconnection to a global organized disturbance at substorm onset. This understanding would be derivable from the statistics of the localized instabilities if, with the influence of the variable solar wind included, a correct statistical–physical model of the plasma sheet multiscale dynamics were available.

[37] **Acknowledgments.** We wish to thank N. Watkins for his friendly attention to our work and useful and detailed advice on the manuscript, T. Lui for providing explanations of his method, G. Consolini for valuable discussion on lifetime distributions, and R. Weigel for comments on a draft. We also thank our referees for their constructive criticisms and helpful recommendations. This work of VU was supported by the Resident Research Associateship Program of the National Research Council, USA.

[38] Arthur Richmond thanks A. Surjalal Sharma and another reviewer for their assistance in evaluating this paper.

References

Angelopoulos, V., C. F. Kennel, F. V. Coroniti, R. Pellat, M. G. Kivelson, R. J. Walker, C. T. Russell, W. Baumjohann, W. C. Feldman, and J. T. Gosling, Statistical Characteristics of Bursty Bulk Flow Events, *J. Geophys. Res.*, *99*(A11), 21,257–21,280, 1994.

Angelopoulos, V., F. S. Mozer, T. Mukai, K. Tsuruda, S. Kokubun, and T. J. Hughes, On the relationship between bursty flows, current disruption and substorms, *Geophys. Res. Lett.*, *26*(18), 2841–2844, 1999a.

Angelopoulos, V., T. Mukai, and S. Kokubun, Evidence for intermittency in Earth's plasma sheet and implications for self-organized criticality, *Phys. Plasmas*, *6*(11), 4161–4168, 1999b.

Bak, P., C. Tang, and K. Wiesenfeld, Self-organized criticality—An explanation of 1/F noise, *Phys. Rev. Lett.*, *59*(4), 381–384, 1987.

Bak, P., C. Tang, and K. Wiesenfeld, Self-organized criticality, *Phys. Rev. A*, *38*(1), 364–374, 1988.

Becker, T., H. Devries, and B. Eckhardt, Dynamics of a stochastically driven running sandpile, *J. Nonlinear Sci.*, *5*(2), 167–188, 1995.

Borodich, F. M., Renormalization schemes for earthquake prediction, *Geophys. J. Int.*, *131*(1), 171–178, 1997.

Borovsky, J. E., R. C. Elphic, H. O. Funsten, and M. F. Thomsen, The Earth's plasma sheet as a laboratory for flow turbulence in high-beta MHD, *J. Plasma Phys.*, *57*, 1–34, 1997.

Brittnacher, M., R. Elsen, G. Parks, L. Chen, G. Germany, and J. Spann, A dayside auroral energy deposition case study using the Polar Ultraviolet Imager, *Geophys. Res. Lett.*, *24*(8), 991–994, 1997.

Carbary, J. F., K. Liou, A. T. Y. Lui, P. T. Newell, and C. I. Meng, "Blob" analysis of auroral substorm dynamics, *J. Geophys. Res.*, *105*(A7), 16,083–16,091, 2000.

Chang, T., Low-dimensional behavior and symmetry-breaking of stochastic-systems near criticality—Can these effects be observed in space and in the laboratory, *IEEE Trans. Plasma Sci.*, *20*(6), 691–694, 1992a.

Chang, T., Path-integrals, differential renormalization-group, and stochastic-systems near criticality, *Int. J. Eng. Sci.*, *30*(10), 1401–1405, 1992b.

Chang, T., Sporadic localized reconnections and intermittent turbulence in the magnetotail, in *Geospace Mass and Energy Flow*, edited by J. L. Horwitz, D. L. Gallagher, and W. K. Peterson, p. 193, AGU, Washington, D. C., 1998.

Chang, T., Self-organized criticality, multi-fractal spectra, sporadic localized reconnections and intermittent turbulence in the magnetotail, *Phys. Plasmas*, *6*(11), 4137–4145, 1999.

Charbonneau, P., S. McIntosh, H.-L. Liu, and T. J. Bogdan, Avalanche models for solar flares (invited review), *Sol. Phys.*, *203*, 321–353, 2001.

Chua, D., G. Parks, M. Brittnacher, W. Peria, G. Germany, J. Spann, and C. Carlson, Energy characteristics of auroral electron precipitation: A comparison of substorms and pressure pulse related auroral activity, *J. Geophys. Res.*, *106*(A4), 5945–5956, 2001.

Consolini, G., Sandpile cellular automata and magnetospheric dynamics, in *Proceedings of the 8th GIFCO Conference, Cosmic Physics in the Year 2000: Scientific Perspectives and New Instrumentation*, edited by S. Aiello, pp. 123–126, Editrice Compositori, Bologna, Italy, 1997.

Consolini, G., and T. S. Chang, Magnetic field topology and criticality in geotail dynamics: Relevance to substorm phenomena, *Space Sci. Rev.*, *95*(1–2), 309–321, 2001.

Consolini, G., M. F. Marcucci, and H. Candidi, Multifractal structure of auroral electrojet index data, *Phys. Rev. Lett.*, *76*(21), 4082–4085, 1996.

Cronin, J. W., The highest energy cosmic rays, in *Unsolved Problems in Astrophysics*, edited by J. E. Bahcall and J. P. Ostriker, pp. 325–339, Princeton Univ. Press, Princeton, N. J., 1997.

Doe, R. A., J. D. Kelly, D. Lummerzheim, G. K. Parks, M. J. Brittnacher, G. A. Germany, and J. Spann, Initial comparison of POLAR UVI and Sondrestrom IS radar estimates for auroral electron energy flux, *Geophys. Res. Lett.*, *24*(8), 999–1002, 1997.

Fairfield, D. H., et al., Earthward flow bursts in the inner magnetotail and their relation to auroral brightenings, AKR intensifications, geosynchronous particle injections and magnetic activity, *J. Geophys. Res.*, *104*(A1), 355–370, 1999.

Freeman, M. P., and C. J. Farrugia, Solar wind input between substorm onsets during and after the October 18–20, 1995, magnetic cloud, *J. Geophys. Res.*, *104*(A10), 22,729–22,744, 1999.

Freeman, M. P., N. W. Watkins, and D. J. Riley, Evidence for a solar wind origin of the power law burst lifetime distribution of the AE indices, *Geophys. Res. Lett.*, *27*(8), 1087–1090, 2000.

Germany, G. A., M. R. Torr, D. G. Torr, and P. G. Richards, Use of FUV auroral emissions as diagnostic indicators, *J. Geophys. Res.*, *99*(A1), 383, 1994.

Germany, G. A., G. K. Parks, M. Brittnacher, J. Cumnock, D. Lummerzheim, J. F. Spann, L. Chen, P. G. Richards, and F. J. Rich, Remote determination of auroral energy characteristics during substorm activity, *Geophys. Res. Lett.*, *24*(8), 995–998, 1997.

Germany, G. A., G. K. Parks, H. Ranganath, R. Elsen, P. G. Richards, W. Swift, J. F. Spann, and M. Brittnacher, Analysis of auroral morphology: Substorm precursor and onset on January 10, 1997, *Geophys. Res. Lett.*, *25*(15), 3043–3046, 1998.

Gleisner, H., and H. Lundstedt, A neural network-based local model for prediction of geomagnetic disturbances, *J. Geophys. Res.*, *106*(A5), 8425–8433, 2001.

Horton, W., and I. Doxas, A low-dimension energy-conserving state space model for substorm dynamics, *J. Geophys. Res.*, *101*(A12), 27,223–27,237, 1996.

Horton, W., and I. Doxas, A low-dimensional dynamical model for the solar wind driven geotail-ionosphere system, *J. Geophys. Res.*, *103*(A3), 4561–4572, 1998.

Hwa, T., and M. Kardar, Avalanches, hydrodynamics, and discharge events in models of sandpiles, *Phys. Rev. A*, *45*(10), 7002–7023, 1992.

Ieda, A., D. H. Fairfield, T. Mukai, Y. Saito, S. Kokubun, K. Liou, C. I. Meng, G. K. Parks, and M. J. Brittnacher, Plasmoid ejection and auroral brightenings, *J. Geophys. Res.*, *106*(A3), 3845–3857, 2001.

Klimas, A. J., D. N. Baker, D. A. Roberts, D. H. Fairfield, and J. Buchner, A nonlinear dynamic analog model of geomagnetic activity, *J. Geophys. Res.*, *97*(A8), 12,253–12,266, 1992.

Klimas, A. J., D. N. Baker, D. Vassiliadis, and D. A. Roberts, Substorm recurrence during steady and variable solar wind driving: Evidence for a normal mode in the unloading dynamics of the magnetosphere, *J. Geophys. Res.*, *99*(A8), 14,855–14,861, 1994.

Klimas, A. J., D. Vassiliadis, D. N. Baker, and D. A. Roberts, The organized nonlinear dynamics of the magnetosphere, *J. Geophys. Res.*, *101*(A6), 13,089–13,113, 1996.

Klimas, A. J., D. Vassiliadis, and D. N. Baker, Data-derived analogues of the magnetospheric dynamics, *J. Geophys. Res.*, *102*(A12), 26,993–27,009, 1997.

Klimas, A. J., V. M. Uritsky, J. A. Valdivia, D. Vassiliadis, and D. N. Baker, On the compatibility of the coherent substorm cycle with the complex plasma sheet, in *5th International Conference on Substorms*, edited by A. Wilson, pp. 165–168, ESA, St. Petersburg, Russia, 2000a.

Klimas, A. J., J. A. Valdivia, D. Vassiliadis, D. N. Baker, M. Hesse, and J. Takalo, Self-organized criticality in the substorm phenomenon and its relation to localized reconnection in the magnetospheric plasma sheet, *J. Geophys. Res.*, *105*(A8), 18,765–18,780, 2000b.

Lui, A. T. Y., S. C. Chapman, K. Liou, P. T. Newell, C. I. Meng, M. Brittnacher, and G. D. Parks, Is the dynamic magnetosphere an avalanching system?, *Geophys. Res. Lett.*, *27*(7), 911–914, 2000.

Lyons, L. R., T. Nagai, G. T. Blanchard, J. C. Samson, T. Yamamoto, T. Mukai, A. Nishida, and S. Kokubun, Association between Geotail plasma flows and auroral poleward boundary intensifications observed by CANOPUS photometers, *J. Geophys. Res.*, *104*(A3), 4485–4500, 1999.

Main, I., Statistical physics, seismogenesis, and seismic hazard, *Rev. Geophys.*, *34*(4), 433–462, 1996.

Malamud, B. D., G. Morein, and D. L. Turcotte, Forest fires: An example of self-organized critical behavior, *Science*, *281*, 1840–1842, 1998.

Munoz, M. A., R. Dickman, A. Vespignani, and S. Zapperi, Avalanche and spreading exponents in systems with absorbing states, *Phys. Rev. E*, *59*(5), 6175–6179, 1999.
Nakamura, R., W. Baumjohann, M. Brittnacher, V. A. Sergeev, M. Kubyshkina, T. Mukai, and K. Liou, Flow bursts and auroral activations: Onset timing and foot point location, *J. Geophys. Res.*, *106*(A6), 10,777–10,789, 2001a.
Nakamura, R., W. Baumjohann, R. Schodel, M. Brittnacher, V. A. Sergeev, M. Kubyshkina, T. Mukai, and K. Liou, Earthward flow bursts, auroral streamers, and small expansions, *J. Geophys. Res.*, *106*(A6), 10,791–10,802, 2001b.
Newell, P. T., K. Liou, T. Sotirelis, and C. I. Meng, Polar Ultraviolet Imager observations of global auroral power as a function of polar cap size and magnetotail stretching, *J. Geophys. Res.*, *106*(A4), 5895–5905, 2001.
Pavlos, G. P., M. A. Athanasiu, D. Kugiumtzis, N. Hatzigeorgiu, A. G. Rigas, and E. T. Sarris, Nonlinear analysis of magnetospheric data, 1, Geometric characteristics of the AE index time series and comparison with nonlinear surrogate data, *Nonlinear Proc. Geophys.*, *6*(11), 51–56, 1999a.
Pavlos, G. P., D. Kugiumtzis, M. A. Athanasiu, N. Hatzigeorgiu, D. Diamantidis, and E. T. Sarris, Nonlinear analysis of magnetospheric data, 2, Dynamical characteristics of the AE index time series and comparison with nonlinear surrogate data, *Nonlinear Proc. Geophys.*, *6*(2), 79–98, 1999b.
Robinson, P. A., Scaling properties of self-organized criticality, *Phys. Rev. E*, *49*(5), 3919–3926, 1994.
Sauvaud, J. A., D. Popescu, D. C. Delcourt, G. K. Parks, M. Brittnacher, V. Sergeev, R. A. Kovrazhkin, T. Mukai, and S. Kokubun, Sporadic plasma sheet ion injections into the high-altitude auroral bulge: Satellite observations, *J. Geophys. Res.*, *104*(A12), 28,565–28,586, 1999.
Sergeev, V. A., K. Liou, C. I. Meng, P. T. Newell, M. Brittnacher, G. Parks, and G. D. Reeves, Development of auroral streamers in association with localized impulsive injections to the inner magnetotail, *Geophys. Res. Lett.*, *26*(3), 417–420, 1999.
Sharma, A. S., Assessing the magnetospheres nonlinear behavior—Its dimension is low, its predictability, *Rev. Geophys.*, *33*, 645–650, 1995.
Sitnov, M. I., A. S. Sharma, K. Papadopoulos, D. Vassiliadis, J. A. Valdivia, A. J. Klimas, and D. N. Baker, Phase transition-like behavior of the magnetosphere during substorms, *J. Geophys. Res.*, *105*(A6), 12,955–12,974, 2000.
Sitnov, M. I., A. S. Sharma, K. Papadopoulis, and D. Vassiliadis, Modeling substorm dynamics of the magnetosphere: From self-organization and self-organized criticality to nonequilibrium phase transitions, *Phys. Rev. E*, *65*(1), 16,116, 2002.
Takalo, J., J. Timonen, and H. Koskinen, Correlation dimension and affinity of AE data and bicolored noise, *Geophys. Res. Lett.*, *20*(15), 1527–1530, 1993.
Takalo, J., J. Timonen, A. J. Klimas, J. A. Valdivia, and D. Vassiliadis, A coupled-map model for the magnetotail current sheet, *Geophys. Res. Lett.*, *26*(19), 2913–2916, 1999.
Tsurutani, B. T., M. Sugiura, T. Iyemori, B. E. Goldstein, W. D. Gonzalez, S. I. Akasofu, and E. J. Smith, The nonlinear response of AE to the IMF Bs driver—A spectral break at 5 hours, *Geophys. Res. Lett.*, *17*(3), 279–282, 1990.
Turcotte, D. L., *Fractals and Chaos in Geology and Geophysics*, 398 pp., Cambridge Univ. Press, New York, 1997.
Uritsky, V. M., and M. I. Pudovkin, Low frequency 1/f-like fluctuations of the AE-index as a possible manifestation of self-organized criticality in the magnetosphere, *Ann. Geophys.*, *16*(12), 1580–1588, 1998.
Uritsky, V. M., A. J. Klimas, J. A. Valdivia, D. Vassiliadis, and D. N. Baker, Stable critical behavior and fast field annihilation in a magnetic filed reversal model, *J. Atmos. Sol. Terr. Phys.*, *63*(13), 1425–1433, 2001a.
Uritsky, V. M., A. J. Klimas, and D. Vassiliadis, Comparative study of dynamical critical scaling in the auroral electrojet index versus solar wind fluctuations, *Geophys. Res. Lett.*, *28*(19), 3809–3812, 2001b.
Uritsky, V. M., A. J. Klimas, and D. Vassiliadis, Multiscale dynamics and robust critical scaling in a continuum current sheet model, *Phys. Rev. E*, *65*(4), 046113-1–046113-5, 2002.
Valdivia, J. A., A. S. Sharma, and K. Papadopoulos, Prediction of magnetic storms by nonlinear models, *Geophys. Res. Lett.*, *23*(21), 2899–2902, 1996.
Valdivia, J. A., D. Vassiliadis, A. J. Klimas, and A. S. Sharma, Modeling the spatial structure of the high latitude magnetic perturbations and the related current system, *Phys. Plasmas*, *6*(11), 4185–4199, 1999.
Vassiliadis, D., A. J. Klimas, D. N. Baker, and D. A. Roberts, A description of the solar-wind magnetosphere coupling based on nonlinear filters, *J. Geophys. Res.*, *100*(A3), 3495–3512, 1995.
Vassiliadis, D., A. J. Klimas, J. A. Valdivia, and D. N. Baker, The *Dst* geomagnetic response as a function of storm phase and amplitude and the solar wind electric field, *J. Geophys. Res.*, *104*(A11), 24,957–24,976, 1999.
Weiss, L. A., P. H. Reiff, J. J. Moses, R. A. Heelis, and B. D. Moore, Energy dissipation in substorms, in *1st International Conference on Substorms (ICS-1)*, pp. 309–317, ESA, Kiruna, Sweden, 1992.
Zesta, E., L. R. Lyons, and E. Donovan, The auroral signature of Earthward flow bursts observed in the Magnetotail, *Geophys. Res. Lett.*, *27*(20), 3241–3244, 2000.

D. Chua and G. Parks, Department of Earth and Space Sciences, University of Washington, Seattle, WA, 98195 USA.

A. J. Klimas, Magnetospheric Physics Laboratory, NASA Goddard Space Flight Center, Code 692, Greenbelt, MD 20771, USA.

V. M. Uritsky, Magnetospheric Physics Laboratory, Institute of Physics, St. Petersburg State University, Russia. (uritsky@geo.phys.spbu.ru)

D. Vassiliadis, USRA, NASA Goddard Space Flight Center, Code 692, Greenbelt, MD 20771, USA.